

See discussions, stats, and author profiles for this publication at: <https://www.researchgate.net/publication/41967709>

Photophysics of the Red Chromophore of HcRed: Evidence for Cis-Trans Isomerization and Protonation-State Changes

ARTICLE in THE JOURNAL OF PHYSICAL CHEMISTRY B · MARCH 2010

Impact Factor: 3.3 · DOI: 10.1021/jp9102146 · Source: PubMed

CITATIONS

9

READS

28

6 AUTHORS, INCLUDING:



Thilak Mudalige

U.S. Food and Drug Administration

29 PUBLICATIONS 389 CITATIONS

SEE PROFILE



Satoshi Habuchi

King Abdullah University of Science and Te...

71 PUBLICATIONS 2,170 CITATIONS

SEE PROFILE



Peter M Goodwin

Los Alamos National Laboratory

129 PUBLICATIONS 2,949 CITATIONS

SEE PROFILE



Frans C De Schryver

University of Leuven

671 PUBLICATIONS 21,236 CITATIONS

SEE PROFILE

Photophysics of the Red Chromophore of HcRed: Evidence for Cis–Trans Isomerization and Protonation-State Changes

Kumara Mudalige,[†] Satoshi Habuchi,[‡] Peter M. Goodwin,[§] Ranjith K. Pai,[†] Frans De Schryver,[‡] and Mircea Cotlet^{*,†}

Center for Functional Nanomaterials, Brookhaven National Laboratory, Mail Stop 735, Upton New York 11973, Department of Chemistry, Katholieke Universiteit Leuven, Celestijnenlaan 200F, Heverlee Leuven B-3001, Belgium, and Center for Integrated Nanotechnologies, Los Alamos National Laboratory, Mail Stop K771, Los Alamos, New Mexico 87545

Received: October 26, 2009; Revised Manuscript Received: February 15, 2010

HcRed is a dimeric intrinsically fluorescent protein with origins in the sea anemone *Heteractis crispa*. This protein exhibits deep red absorption and emission properties. Using a combination of ensemble and single molecule methods and by varying environmental parameters such as temperature and pH, we found spectroscopic evidence for the presence of two ground state conformers, trans and cis chromophores that are in thermal equilibrium and that follow different excited-state pathways upon exposure to light. The photocycle of HcRed appears to be a combination of both kindling proteins and bright emitting GFP/GFP-like proteins: the trans chromophore undergoes light driven isomerization followed by radiative relaxation with a fluorescence lifetime of 0.5 ns. The cis chromophore exhibits a photocycle similar to bright GFPs and GFP-like proteins such as enhanced GFP, enhanced YFP or DsRed, with radiative relaxation with a fluorescence lifetime of 1.5 ns, singlet–triplet deactivation on a microsecond time scale and solvent controlled protonation/deprotonation in tens of microseconds. Using single molecule spectroscopy, we identify trans and cis conformers at the level of individual moieties and show that it is possible that the two conformers can coexist in a single protein due to the dimeric nature of HcRed.

1. Introduction

Fluorescent proteins with origins in the *Aequorea victoria* jellyfish and in corals provide emission colors covering the visible spectral range from blue to deep red.^{1–3} These proteins have been intensively used as fluorescent reporters in a wide variety of cell and molecular biology applications, including intracellular localization, ratiometric reporters for pH, tags for protein expression, protein-folding reporters and protein–protein interaction studies based on fluorescence microscopy.^{1,4,5} More recently, photo switchable proteins known under the name of “kindling” proteins have attracted interest due to their potential use in conjunction with recently developed super-resolution fluorescence microscopies, methods capable of breaking down the diffraction limit encountered in conventional confocal microscopy.^{6,7} Kindling proteins reversibly commute their fluorescence under light exposure between an “on” fluorescent state and an “off” nonfluorescent state.^{8–12}

Brightness of the green fluorescent protein (GFP) of various GFP mutants and of some GFP-like proteins (proteins with origins in corals) has been associated with a fluorescent chromophore adopting a cis, coplanar orientation. Crystallographic studies stand behind this assumption for proteins such as wild-type GFP, enhanced GFP (EGFP), enhanced yellow fluorescent protein (EYFP), DsRed, or Venus.^{13–17} A cis orientation is achieved by tight encapsulation of the chromophore inside an eleven stranded β -barrel fold and with

contribution of a complex hydrogen bonding network composed of amino-acids and water molecules. This tight encapsulation locks the chromophore in conformations for which nonradiative relaxation is mostly suppressed,^{1,18} thus providing a high brightness for the protein itself, as opposed to synthetic analogues of the GFP chromophore that lack fluorescence.¹⁸ Chromoproteins such as Rtns5 and hcCP have trans-oriented, nonplanar, nonfluorescent chromophores.² An exception is the tetrameric eqFP611, a bright emitting red fluorescent protein from *Entomarea quadricolor* with a trans-oriented chromophore that possesses a relatively high quantum yield of fluorescence.^{19,20} Within the class of kindling proteins,^{12,21,22} the *Anemonia sulcata* asFP595 chromophore adopts a trans orientation for the off (nonfluorescent) state and a cis orientation for the on (fluorescent) state.^{9,12,23,24}

Here we report ensemble and single molecule spectroscopic data in relation to the photocycle of HcRed, a dimeric protein generated by coupled site-directed and random mutagenesis from a chromoprotein (hcCP) cloned from the sea anemone *Heteractis crispa*.^{2,4,25} Within the class of GFP-like proteins, HcRed is remarkable by its deep red absorption and emission spectral properties, absorption peaking at 590 nm and fluorescence peaking at 645 nm. Here we show that HcRed has a complex photocycle that resembles that of both kindling proteins and of bright emitting GFPs and GFP-like proteins (e.g., EGFP, EYFP, DsRed). This photocycle involves thermally equilibrated ground-state trans and cis chromophores undergoing distinct excited state pathways, including light induced trans–cis isomerization and solvent controlled protonation/deprotonation. Our study, while contributing to the photophysical characterization of a commercially available biomarker for which little biophysical information is available but needed, especially in quantitative

* To whom correspondence should be addressed. E-mail: cotlet@bnl.gov. Phone 631-344-7778. Fax 631-344-7765.

[†] Brookhaven National Laboratory.

[‡] Katholieke Universiteit Leuven.

[§] Los Alamos National Laboratory.

assays based on fluorescence microscopy,²⁶ may stimulate future efforts in designing new variants of HcRed with either improved kindling behavior or with increased brightness at longer wavelengths.

2. Materials and Methods

2.1. Protein Purification. Details on the cloning, expression, and purification are reported elsewhere.² For solution experiments, HcRed was diluted in phosphate buffered saline (PBS, pH 7.4, Dulbecco) to 10^{-6} M for ensemble spectroscopic experiments and to 10^{-8} M for fluorescence correlation spectroscopy. For pH dependent spectroscopy, HcRed was diluted in a series of mixture buffers (TRIS, MOPS, MES, or citrate buffer) with the pH adjusted by adding small amounts of HCl. For single molecule experiments, proteins were immobilized (from a stock solution of 10^{-8} M in PBS) in polyacrylamide gel (2–4% w, Sigma Aldrich), with the gel sandwiched between two transparent cover glasses.

2.2. Ensemble Spectroscopy. Absorption and fluorescence spectra were recorded with a Perkin-Elmer Lambda 25 spectrophotometer and a Spex Fluorolog 1500 fluorimeter (Spex Industries, Metuchen, NJ). Fluorescence decays were measured by the time-correlated single photon counting (TCSPC) method by using the 570 nm excitation light provided by a pulsed laser system (Spectra Physics, 80 MHz, 120 fs pulse width). Fluorescence decays were measured at magic angle, with a dwell time of 4 ps, by a detection system composed of a microchannel plate photomultiplier (Hamamatsu R3809U-50, Japan), a monochromator (Jobin Yvon, H-10 VIS) and a TCSPC PC card (Becker-Hickl SPC 630, Germany). Fluorescence decays were analyzed by forward convolution of the instrument function of the TCSPC setup (~ 45 ps fwhm) with an exponential model by using the Fluofit Pro software (Picoquant, GmbH, Germany). The contribution of the fluorescence lifetimes reported herein was calculated either as a weighted contribution, $\alpha_i = A_i \tau_i / \sum A_i \tau_i$, with A_i and τ_i the pre-exponent factor and fluorescence lifetime, respectively, or as a nonweighted contribution, $a_i = A_i / \sum A_i$.

2.3. Fluorescence Correlation Spectroscopy (FCS). FCS experiments were performed with the 594 nm light from a He–Ne laser (Melles Griot) using a confocal inverted microscope (Olympus IX 71) with a water immersion lens (Olympus Japan, 1.2 NA, 60 \times). Fluorescence collected by the same lens was isolated from the excitation laser by a dichroic mirror (DRLP610, Chroma Technologies), a band-pass filter (650/50HQB, Chroma), spatially filtered with a 75 μ m pinhole, split by a 50/50% beam splitter and imaged onto two single photon counting modules (SPAD, SPCM AQR 14, Perkin-Elmer). The signals from the SPADs were cross-correlated by a fast hardware correlator (ALV5000/E FAST, ALV GmbH). Rhodamine B in water (10^{-8} M concentration) was used to calibrate the probe volume of the FCS apparatus.²⁷ FCS curves were analyzed using the IgorPro Wavemetrics software.

2.4. Single-Molecule Fluorescence Spectroscopy. Individual immobilized HcRed molecules were imaged with a confocal inverted microscope (Olympus IX71) equipped with an oil immersion lens (Olympus Japan, 1.4 NA, 100 \times) and by using a piezo-scanning stage (MadCity Lab H-100). For optical excitation we used the 570 nm pulsed light. Fluorescence was collected by the same lens, isolated from the excitation laser by the same combination dichroic/bandpass filters as for FCS, spatially filtered by a 100 μ m pinhole, and focused on a single SPAD. The signal from the SPAD was registered by a TCSPC PC card (Becker Hickl, SPC630, Germany) operated in the FIFO (first-in, first out) mode. This particular mode allows each detected photon to be time-stamped with respect to the excitation

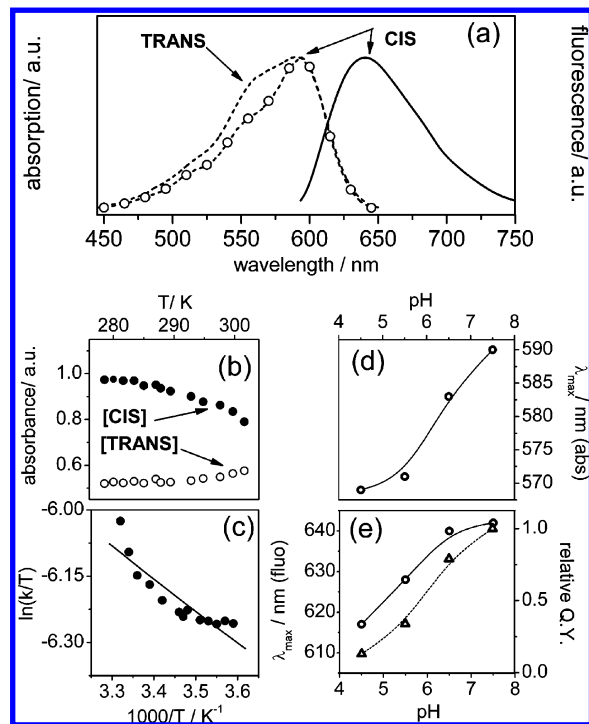


Figure 1. (a) Room-temperature (20 °C) absorption (dashed line), fluorescence excitation ($\lambda_{\text{det}} \sim 650$ nm, dashed line and circles) and fluorescence emission ($\lambda_{\text{exc}} \sim 590$ nm, solid line) spectra of HcRed in phosphate buffered saline (PBS, pH 7.5). (b) Temperature-dependence of the peak absorbances of the bands corresponding to the cis (dots) and trans (circles) forms of HcRed chromophore. Data are normalized to the value of the peak absorbance of the cis band at 5 °C. Data in panel b were estimated by decomposing the temperature-dependent absorption spectra of HcRed (Figure.S1, Supporting Information) by Gaussians peaking at around 590 nm (cis form) and 565 nm (trans form). (c) Plot of $\ln(k/T)$ vs $1/T$ (dots) and linear fit (black line), with $k = [\text{TRANS}]/[\text{CIS}]$, with [TRANS] and [CIS] data from panel b. (d) pH dependence of the absorption peak wavelength of HcRed. (e) pH dependence of the emission peak wavelength (solid line and circles) and fluorescence quantum yield (dashed line and triangles). Data were normalized to values corresponding to pH 7.5.

pulse (microtime) and with respect to the previously detected photon (macrotime). Postprocessing of this temporal information allows construction of time-trajectories of single molecule fluorescence intensity (by using macrotime information) and lifetime (by using microtime information).²⁸ Here, single molecule fluorescence decay times were estimated by the maximum likelihood estimation method^{28–30} from decay histograms of 500 photons by forward convolution of the response function of the single molecule instrument (~ 350 ps) with a single exponential model.

3. Results

3.1. Room-Temperature Spectroscopy. The absorption spectrum of HcRed features a main peak at 590 nm and a shoulder at 565-nm (Figure 1a, dashed line; HcRed dissolved in phosphate buffered saline, PBS). The extinction coefficient of HcRed measured at the peak wavelength is $120\,000\text{ M}^{-1}\text{ cm}^{-1}$. The fluorescence of HcRed ($\lambda_{\text{exc}} = 590$ nm) is weak (quantum yield of fluorescence in PBS ~ 0.05) and spectrally broad, with a main peak at 645 nm (Figure 1a, solid line). It is noteworthy that the excitation spectrum of HcRed (detection at 645-nm) has a peak at 590 nm but lacks a shoulder at 565 nm (see Figure 1a, spectrum as dashed line and dots). The fluorescence of HcRed detected at the main emission peak

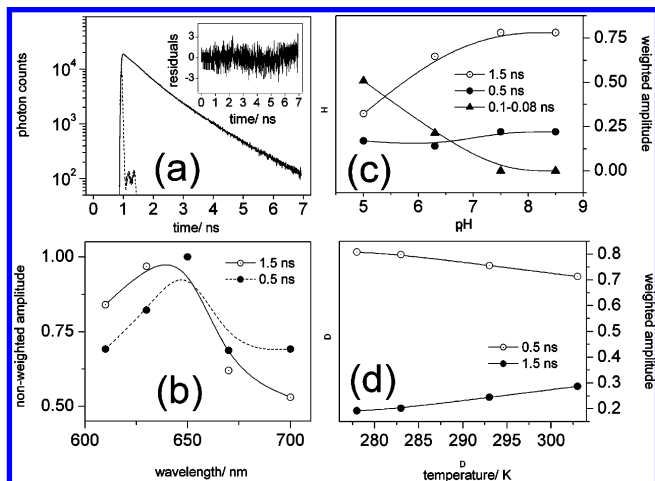


Figure 2. Time-resolved fluorescence spectroscopy of HcRed with 570 nm excitation. (a) Room-temperature fluorescence decay of HcRed in PBS (20 °C) detected at 650 nm and biexponential fit (gray line) with fluorescence lifetimes of 1.5 ns (78%) and 0.5 ns (22%). Shown in gray dotted line is the response function of the instrument. Inset shows the residuals of the fit. (b) Wavelength dependence of the nonweighted amplitudes (normalized to unity) of the room-temperature fluorescence lifetimes of HcRed in PBS. (c) pH dependence of the weighted amplitudes of the fluorescence lifetimes of HcRed. Note the additional fluorescence lifetime of ~ 0.1 ns present at low pH. (d) Temperature-dependence of the weighted amplitudes of the fluorescence lifetimes of HcRed in PBS, pH 7.4.

decays biexponentially with lifetimes of 0.5 ns (22% weighted amplitude) and 1.5 ns (78% weighted amplitude) (Figure 2a). The corresponding weighted amplitudes of the two lifetimes change very little when measured across the emission spectrum, instead, the corresponding nonweighted amplitudes follow the profile of the fluorescence spectrum of the protein (see Figure 2b).

3.2. Temperature-Dependent Spectroscopy. The absorption spectrum of HcRed is sensitive to changes in temperature; by increasing the temperature from 5 to 30 °C, the main peak at 590 nm decreases in intensity and the 565 nm shoulder increases. This change with the temperature is reversible and features an isosbestic point at 578 nm (see Figure.S1 in Supporting Information). This change with temperature was analyzed by decomposing the absorption spectra of HcRed (Figure.S1 in Supporting Information) into Gaussians peaking at 590 and 565 nm, respectively (see Figure 1b). In contrast, both the excitation spectrum (detection at 645 nm) and the emission spectrum (excitation at 590 nm) are shape-insensitive to changes in temperature. Temperature affects the contributions of the fluorescence lifetimes of HcRed (weighted amplitudes); the long lifetime (1.5 ns) decreases in contribution with increasing temperature and, correspondingly, the short lifetime (0.5 ns) increases (see Figure 2d).

3.3. pH-Dependent Spectroscopy of HcRed. The absorption and fluorescence spectra of HcRed are sensitive to changes in pH; from pH 8.5 to 4.5, the main absorption peak shifts from 590 to 568 nm (Figure 1d and Figure.S2, Supporting Information) and a new band appears at 450 nm at pH 4.5 (Figure.S2, Supporting Information). Changing the pH affects the emission properties of HcRed; as the pH decreases from 8.5 to 4.5, the main fluorescence peak shifts from 645 to 612 nm (Figure 1e, line plus circles) and the quantum yield of fluorescence drops almost 9-fold (Figure 1e, line plus triangles). At low pH (pH < 6.5), we detect an additional fast lifetime component with a value of 0.08–0.1 ns, depending on the pH value (see Figure 2c) and with a contribution that increases toward acid pH.

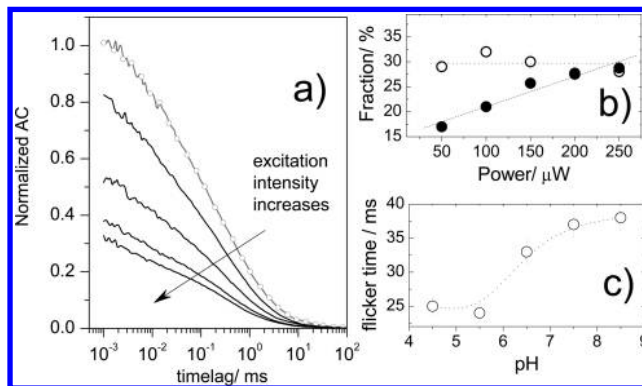


Figure 3. Fluorescence correlation spectroscopy of HcRed in PBS using 594 nm excitation. (a) Autocorrelations of the fluorescence intensity for HcRed at various excitation powers. The AC curve shown with line and dots corresponds to an average power at the sample of 50 μ W, and the arrow indicates increase in the average excitation power, from right to left, in steps of 50 μ W. The AC curve recorded at 50 μ W is normalized to unity. The rest of the AC curves are normalized with the same factor as the AC curve recorded at 50 μ W. (b) Excitation power dependence of the contributions of the fast (3 μ s, dots) and slow (43 μ s, circles) fluorescence flickers of HcRed. Also shown are fits (dashed lines). (c) pH dependence of the slow fluorescence flicker of HcRed in PBS. Data in panels b and c are represented with error bars accounting for 10% error in the estimate of the corresponding parameters.

3.4. Fluorescence Correlation Spectroscopy. Fluorescence correlation spectroscopy (FCS) measures the second order correlation of the fluorescence intensity

$$AC(\tau) = \langle \delta I(t) \delta I(t + \tau) \rangle / \langle I^2(t) \rangle \quad (1)$$

with $\delta I(t) = I(t) - \langle I \rangle$ the time-dependent fluctuation of the fluorescence signal (intensity).^{31–33} FCS relies on the detection of the fluorescence emitted by molecules diffusing freely in and out of a diffraction-limited laser focus. Fluctuations in the fluorescence signal can originate from diffusion, photodynamics (e.g., singlet–triplet transitions, isomerization), or from chemical reactions (e.g., protonation–deprotonation) involving a particular fluorescent molecule or protein. For a simple organic dye, such fluctuations originate from translational diffusion and sometimes from visitations to the triplet state (dark or non-emissive state), for example, singlet–triplet transitions.^{27,31,32} In this case the $AC(\tau)$ is described by

$$AC(\tau) = N^{-1} \frac{1}{(1 + \tau/\tau_{\text{Diff}})[1 + (r_0/\omega_0)^2(\tau/\tau_{\text{Diff}})]^{1/2} [1 + (F_T/(1 - F_T))\exp(-\tau/\tau_T)]} \quad (2)$$

Here N is the average number of molecules in the excitation volume, τ_{Diff} is the diffusion time, r_0 and ω_0 are the radial and axial dimensions of the excitation volume, respectively, and F_T and τ_T are the fraction of molecules in the triplet state and the triplet lifetime, respectively. Figure 3a (decay shown in gray line with open dots) is the normalized AC of HcRed in PBS recorded with 594 nm excitation (average power 50 μ W). This AC is best fit with a kinetic model comprised of a translational diffusion component and two fluorescence flickers F_1 , τ_1 and F_2 , τ_2 :

$$AC(\tau) = N^{-1} \frac{1}{(1 + \tau/\tau_{\text{Diff}})[1 + (r_0/\omega_0)^2 (\tau/\tau_{\text{Diff}})]^{1/2}} \prod_{i=1,2} [1 + (F_i/(1 - F_i))\exp(-\tau/\tau_i)] \quad (3)$$

Equation 3 describes reversible switching of the protein chromophore between an emissive state and two nonemissive (dark) states.^{32,34–36} This AC has in addition to a diffusion time $\tau_{\text{Diff}} \sim 285 \mu\text{s}$ two flicker lifetimes $\tau_1 \sim 3 \mu\text{s}$ (contribution $F_1 \sim 16\%$) and $\tau_2 \sim 43 \mu\text{s}$ (contribution $F_2 \sim 29\%$). For this particular excitation wavelength and for an excitation power of $50 \mu\text{W}$, HcRed exhibits a molecular brightness (detected photons per single protein) $\langle \epsilon \rangle = N^{-1}\langle I \rangle \sim 10 \text{ kHz}$. To determine the nature of the two fluorescence flickers, we investigated their pH- and excitation intensity dependence.^{32,34,37} By increasing the excitation power at the sample from 50 to $250 \mu\text{W}$, we found the fast flicker to increase only in contribution (from 16 to 30%, see Figure 3b) while its lifetime value remained constant. The slow flicker remained unaffected by excitation intensity changes, both in lifetime value and contribution (see Figure 3b). Changes in the bulk pH (from 8.5 to 4.5) did not affect the fast fluorescence flicker fraction or lifetime. The slow flicker was affected by changes in pH with its corresponding lifetime decreasing in value toward acid pH (see Figure 3c) but without noticeable changes in its contribution. We did not observe significant dependence in the molecular brightness of HcRed on pH.

3.5. Single molecule spectroscopy. We used time-resolved single molecule fluorescence detection to probe the dynamics of fluorescence emitted by individual HcRed proteins immobilized in water filled pores of polyacrylamide gels (2–4% w). Distributions of single molecule fluorescence properties from HcRed are shown in Figures 4a,b. These data were compiled from ~ 50 individual HcRed proteins, each excited with 570-nm pulsed light at an average power of $2 \mu\text{W}$. It is noteworthy that all the single molecule fluorescence property distributions indicate heterogeneity in the probed population, suggesting the presence of two types of single emitting species, dim and bright proteins (see below). The distribution of the average photon count rate per protein (see Figure 4a) is bimodal with peaks at ~ 130 and 300 photoncounts/10 ms. Figure 4b is a plot of the average photon count rate against the survival time for individual HcRed proteins. This dependence can be described by a biexponential decay function $A(t) = \sum A_i \exp(-t/T_{si})$, with $i = 1,2$ (see Figure 4b, full line) with survival times, $T_{s1,2} \sim 1.4$ and 40 s . Accordingly, these data suggest strong anticorrelation between molecular brightness and photostability of individual HcRed protein moieties.

The measured probability distribution of the single molecule fluorescence lifetimes of individual HcRed molecules (Figure 4c) can be rationalized as bimodal with mean lifetimes close in value to the lifetimes estimated by ensemble solution spectroscopy in PBS. We found, on average, bright fluorescing proteins to exhibit long lifetimes, around a mean value of 1.5 ns and dim fluorescing proteins exhibiting short lifetimes around a mean value of 0.7 ns (see Figure 4c). Figure 5 shows representative time trajectories of fluorescence lifetimes measured from individual HcRed proteins (Figure 5, left panels) and their corresponding probabilities (Figure 5, right panels). Within these time trajectories we identified single proteins exhibiting either “long” fluorescence lifetimes (Figure 5a, average lifetime 1.4 ns) or “short” fluorescence lifetimes (Figure 5b, average lifetime 0.8 ns), or single proteins switching from “long” lifetimes to “short” lifetimes (Figure 5c, average lifetimes 0.8 and 1.4 ns)

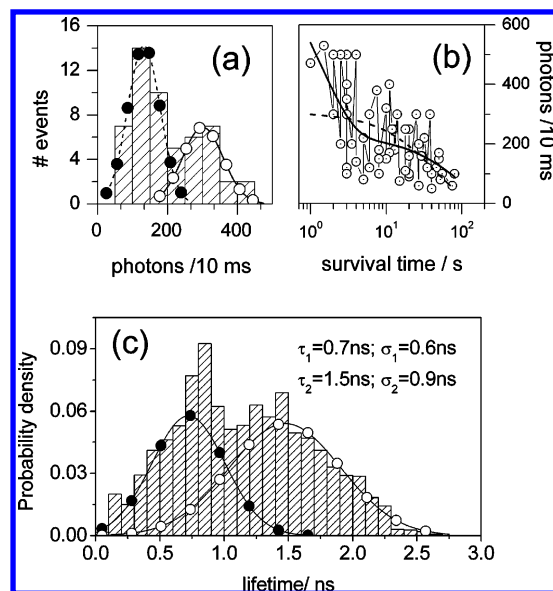


Figure 4. Distributions of single molecular fluorescence parameters of HcRed proteins immobilized in polyacrylamide gel (2–4% w). Data were recorded from 50 individual proteins using 570 nm pulsed laser excitation at an average power $2 \mu\text{W}$. (a) Histogram of the average photon count rate per single protein (dwelt time 10 ms) and Gauss fits (dashed line and dots, solid line and circles) with mean values 130 and 300 photons/ 10 ms . (b) Average photon count rate vs survival time for single HcRed proteins. Also shown are a biexponential fit (solid line) with time constants of 1.4 and 40 s and a single exponential fit (dashed line) with time constant of 20 s . (c) Distribution of single molecule fluorescence lifetime of HcRed and bimodal Gauss fit (mean values 0.7 and 1.5 ns). Each data point in this distribution is a single exponential lifetime estimate by the maximum likelihood estimation method from decay histograms of 500 photons.

or proteins alternating between “long” and “short” lifetimes (Figure 5d, average lifetime of 1.1 ns).

4. Discussion

4.1. Overview. The light absorption and/or fluorescent properties of GFP and of GFP-like proteins and chromoproteins arise from an extended conjugated π -system comprising a cyclic tripeptide chromophore, for example, Ser-Tyr-Gly for GFPs,¹⁶ Gln-Tyr-Gly for DsRed,^{13,38} or Glu-Tyr-Gly for HcRed.²⁵ Chromophore formation in these proteins is autocatalytic, requiring no cofactors, but only the presence of molecular oxygen.^{1,38,39} For GFP-like proteins exhibiting red-shifted spectroscopic properties, the conjugated π -system of the chromophore extends further by the formation of an acylimine bond.^{13,25,38} Tight encapsulation of the chromophore inside the eleven-stranded β -barrel plays an important role in defining the fluorescence properties of these proteins.¹⁸ Bright emitting GFPs and GFP-like proteins have chromophores with cis-oriented, planar conformations, while most of the chromoproteins have trans oriented, nonplanar chromophores. Kindling proteins (e.g., asFP595) are photoswitchable proteins which can be transferred from a nonfluorescent “off” state to a fluorescent “on” state and back by exposure to green and blue light, respectively. Photoactivation involves trans–cis isomerization of the chromophore, with the “off” state corresponding to a trans oriented, nonplanar and nonfluorescent chromophore and the “on” state corresponding to a cis oriented, planar and fluorescent chromophore.^{9,10,12,24,40} It has been suggested that such isomerization might be mediated by the chromophore environment, in particular by a nearby amino acid participating in the chromophore stabilization and possessing ionizable side chain that would act as a titrating

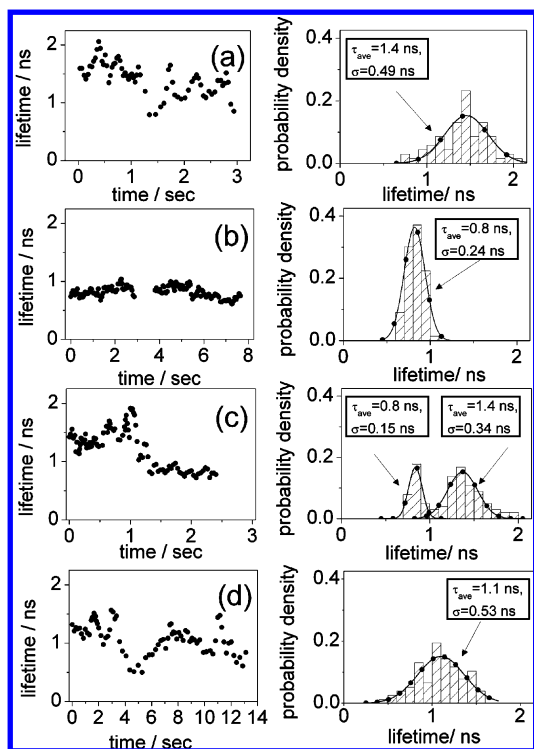


Figure 5. (a–d). Representative time trajectories (left panels) and the corresponding normalized probability distributions (right panel) of the fluorescence lifetimes recorded from single HcRed proteins immobilized in polyacrylamide gels. Distributions shown in right panels include fits according to a Gauss model.

point.⁴¹ In this assumption, isomerization could be driven, within the same protein, by both pH and illumination.

The crystal structure of HcRed²⁵ indicates that the chromophore is a tripeptide Glu64–Tyr65–gly66 containing the 5-[(4-hydroxyphenyl)methylene]-imidazolinone group which is common to GFPs and to GFP-like proteins such as DsRed or EQFP611. π -stacking of HcRed chromophore (the aromatic ring) with a nearby His174 residue extends the chromophore conjugation, resulting in deep red absorption and emission properties when compared to other GFP-like proteins like DsRed or EQFP611. According to ref 25, HcRed chromophore is rather mobile inside the barrel, adopting both trans nonplanar and cis coplanar conformations, and with fluorescence emitted by the cis chromophore. At the level of an individual protein, HcRed occurs as a dimer.^{25,42} Because of the close proximity of the chromophores within a dimer and of the spectral overlap between the absorption and emission spectra (see Figure 1a), intraprotein resonance energy transfer becomes possible,⁴² similar as reported for the tetrameric DsRed.^{35,43–45}

We next interpret our spectroscopic data to account for a limiting model involving cis and trans chromophores and isomerization mediated by chromophore environment^{9,10,25,41} and we demonstrate identification of these conformers at the level of a single protein.

4.2. Evidence for Cis–Trans Isomerization in Solution.

The low energy region of the absorption spectrum of HcRed is defined by two ground state species that absorb at 590 and 565 nm and which are in thermal equilibrium. The temperature dependence of the absorption spectrum of HcRed (see Figure S1, Supporting Information), in particular the temperature dependency of the 590 and 565-nm peak absorbances (see Figure 1b,c, plot of $\ln(k/T)$ vs $1/T$ with k an equilibrium constant calculated with data from Figure 1c), suggests a reversible reaction of the

type A(590 nm) \leftrightarrow B(565 nm) with A, B ground state species in thermal equilibrium. Of the two ground-state species, only one is fluorescent ($\lambda_{\text{em}} \sim 645$ nm), and this is because the emission spectrum of HcRed is (shape) insensitive to changes in temperature. Since for a single fluorescent species the absorption and excitation profiles must coincide, we attribute the fluorescence of HcRed to the ground state species absorbing at ~ 590 nm. In this assumption, and in connection with reference 25 the cis chromophore (C) absorbs at 590 nm and fluoresces at 645 nm and the trans chromophore (T) absorbs at 565 nm and is nonfluorescent.

The fluorescence of HcRed measured at room temperature is biexponential with lifetimes of 1.5 ns (78% weighted contribution) and 0.5 ns (22%). These lifetimes are steady in their weighted contributions across the emission spectrum of the protein. However, their nonweighted contributions follow closely the profile of the emission spectrum (see Figure 2b), suggesting that the two lifetimes belong to two distinct species that are electronically similar (they have similar emission spectra) but possess different fluorescence quantum yields. By increasing the temperature, the contribution of the short lifetime increases (see Figure 2d). Because an increase in temperature shifts the ground state equilibrium toward the population with trans (T) chromophores, the short lifetime (0.5 ns) should be related to an excited state that originates upon the optical excitation of the T chromophore. Since the fluorescence of HcRed must result from an excited cis state,²⁵ optical excitation of the T chromophore must be followed by trans–cis isomerization, a photoswitch that we believe is mediated by the chromophore environment, presumably an amino acid involved in the chromophore stabilization and that can ionize under illumination. Such a scenario has been proposed for *Aequorea victoria* GFP with residue Glu222 as part of the photoswitching mechanism (excited-state proton transfer)¹⁵ for some GFP-like proteins (light-induced cis–trans isomerization in Dronpa⁴⁶ and DsRed⁴⁷ mediated by residues Glu211 and Glu215, respectively) and chromoproteins (pH and light induced trans–cis isomerization in Rtms5(H146S)⁴¹ mediated by residue Glu215). The excited cis species created via the photoswitch decays with a fluorescence lifetime of 0.5 ns. Optical excitation of cis (C) chromophore is followed by radiative deactivation with a lifetime of 1.5 ns. The two excited cis states are electronically (spectrally) similar but differ in fluorescence lifetimes/quantum yields. Presumably, the cis state originating from photoisomerization is an unrelaxed cis chromophore and we shall call this a cis nonrelaxed state (CN*, with * denoting an excited state). CN* is electronically similar to C* but environmentally closer to T*. A similar nonrelaxed state has been suggested for *Aequorea victoria* GFP in order to explain the photocycle of that particular protein.⁴⁸ Photoswitching involving cis–trans isomerization of the protein chromophore has been suggested for GFP (EGFP, S65T)⁴⁹ for several GFP-like proteins including kindling proteins,^{9,12} DsRed,⁴⁷ and a dimeric variant of eqFP611⁵⁰ and for a chromoprotein variant Rtms5(H146S).⁴¹ Alternatively, one might consider that the two fluorescence lifetimes of HcRed relate to two ground state cis conformations that are in equilibrium and that emit with different fluorescent lifetimes/quantum yields, similar as suggested for a cyan variant of GFP.⁵¹ However, the temperature and pH dependent spectroscopy and the single molecule spectroscopy of HcRed argue in favor of a photophysical model involving photoswitching accompanied by trans–cis isomerization (see below).

4.3. pH-Dependent Spectroscopy of HcRed. The photophysical properties of many GFPs are highly dependent on the

pH in the range 4 to 8 and often linked to the pK_a of the protein chromophore.^{52–55} By contrast, GFP-like proteins such as DsRed and EqFP611 show very little changes in their photophysics with the pH, except for alkaline pH.⁴¹ This behavior has been attributed to the low pK_a of their chromophores.^{20,38} For HcRed, from the pH-dependent spectroscopic data reported here it appears that the only state that reacts to bulk protonation in the pH range 8.5–4.5 is the C chromophore. Indeed, the intensities of the absorption and emission peaks, the quantum yield of fluorescence and the contribution of the fluorescence lifetime associated with the C* state, all diminish toward acid pH (see Figure 1d,e and Figure 2c). This suggests that C is an anionic state that undergoes protonation by the bulk solvent, converting into a protonated chromophore that absorbs at around 450 nm (see Supporting Information, Figure.S1). Protonated chromophores with absorption in the blue spectral regions have been reported for GFP-like proteins.^{47,56} The pH dependence of the fluorescence quantum yield (see Figure 2c) suggests a pK_a of 5.5–6 for the C chromophore. By the contrary, the T chromophore seems to be unaffected by changes in the bulk pH; T chromophore's absorption peak and related fluorescence lifetime contribution remain steady in the pH range 8.5–4.5. This suggests a low pK_a value for the T chromophore, below 4.5, similar to chromophores of some GFP-like proteins like DsRed³⁸ and EqFP611.²⁰ At acid pH, the fluorescence of HcRed is weak, peaking at ~612 nm (see Figure.S2 in Supporting Information) and exhibiting an additional fast fluorescence lifetime component (0.1–0.08 ns). Because at acid pH the C chromophore becomes protonated, the residual fluorescence detected from HcRed at ~620 nm must originate from the excited T chromophore (T*).

4.4. Dark States in HcRed. In the assumption that the fluorescence of HcRed is related to a cis chromophore, any fluorescence flicker detected by FCS will reflect the photodynamics of this particular chromophore conformation. The brightness of HcRed, as estimated by FCS, is independent of changes in bulk pH. This is in agreement with FCS probing a single emitting species (cis chromophore). At pH 7.4, the cis chromophore exhibits two fluorescence flickers of 3 and 43 μ s when excited with 50 μ W at 594 nm. The contribution of the fast fluorescence flicker increases at higher excitation intensity. This intensity-dependent flicker is likely due to singlet–triplet (intersystem crossing) transitions of the cis chromophore and it has been observed for bright variants of GFP (enhanced GFP), for DsRed and for some organic dyes.^{27,32,34,37,43,57} The slow fluorescence flicker is insensitive to changes in excitation intensity but reacts to changes in the bulk pH, at least in its lifetime value (see Figure 3c). Similar processes have been observed for some GFP mutants^{27,32,34–36} and attributed to ground-state protonation/deprotonation controlled by the bulk solvent. However, for those particular mutants, the slow flicker was found to react to changes in pH both in contribution and lifetime value. Given that the cis chromophore of HcRed has a $pK_a \sim 5.5$ –6, protonation/deprotonation by bulk pH might be indeed the source of the slow flicker. However, we do not exclude that this slow fluorescence flicker might be in fact a combination of both protonation/deprotonation and ground-state isomerization, as both trans and cis chromophores of HcRed are in thermal equilibrium in the ground state. In fact, a slow flicker component due to ground-state isomerization might explain why we do not detect considerable changes in the contribution of the slow flicker of HcRed when the bulk pH changes over a large range.^{32,34} Presumably, isomerization can be both pH-driven and light-driven in the same protein, as suggested for the chromoprotein Rtms(H146S).⁴¹ Whether or

not this is the case of HcRed, it is hard to predict by the FCS data reported here. This puzzle might be solved with the help of temperature-dependent FCS experiments.

4.5. Single Molecule Demonstration of Trans–Cis Isomerization. The single molecule distributions shown in Figures 4 a–b are a clear indication of the heterogeneity existent in the population of individual HcRed dimer proteins. They all point to the presence of two subpopulations: bright fluorescent proteins exhibiting long fluorescence lifetimes and for which the chromophore is in a cis conformation, and dim fluorescing proteins emitting with short lifetimes and for which the emitting chromophore originated from a ground state T conformation prior to optical excitation. The time trajectories of the fluorescence lifetimes measured from individual HcRed proteins shown in Figure 5 are examples of the various conformers that can be present in an individual HcRed dimer. We find individual proteins that exhibit only long lifetimes and therefore emission from the C* state only (Figure 5a), indicating that we optically probe a protein having the emitting chromophore in a C* state (cis orientation in the ground state). Figure 5b is an example of a single protein exhibiting emission from the CN* state only, therefore having a chromophore with trans orientation in the ground state. Figure 5 panels c and d are examples of single proteins exhibiting emission from both C* (cis ground state) and CN* (trans ground state) states, either in a successive way (Figure 5c) or alternating (Figure 5d). The presence of both cis and trans conformers in a single protein is not unlikely since HcRed is known to occur as a dimer.^{25,42} In fact, Figure 5c is a demonstration of the dimeric state of HcRed,⁴² as it contains both types of chromophores, C and T, and it shows sudden change in the fluorescence lifetime from the C* state to the CN* state. For the case of single proteins alternating between the cis and trans states, an estimate of the time scale of the fluctuation of the single molecule fluorescence lifetime by the a photon by photon analysis method that is suitable for single molecule systems experiencing conformational changes,⁵⁸ suggests dynamics in the time scale of tens of milliseconds (see Supporting Information, Figure.S3 and details on the photon by photon analysis in Supporting Information). This indicates a slow interconversion between the cis and trans forms, about 3 orders of magnitude than eventually predicted by the solution FCS experiments. One possible explanation is that for immobilized proteins, the polymer matrix might restrict movement of the chromophore inside the protein barrel, leading to partial freezing of the chromophore in a given conformation and presumably to a decrease in the rate for ground state isomerization. Such polymer–chromophore interactions affecting the rigidity of a single chromophore have been observed for autofluorescent proteins,^{28,47} fluorescently labeled proteins, and organic dyes^{59,60} immobilized in polyacrylamide gels.

5. Conclusion

HcRed, a GFP-like protein with origins in the sea anemone *Heteractis crispa* and with deep red absorption and emission properties, was found to exhibit complex photophysics including conformationally different chromophores and photoswitching involving trans–cis isomerization. Using a combination of ensemble and single molecule methods and by varying environmental parameters (temperature, pH), we found spectroscopic evidence for the presence of two ground state conformers, trans and cis states that are in thermal equilibrium and which follow different excited state pathways upon illumination. In an attempt to explain the photocycle of HcRed on the basis on the spectroscopic results reported here and in agreement with the

crystal structure of HcRed,²⁵ we have proposed a model in which the trans chromophore undergoes light driven trans–cis isomerization with the “help” of chromophore’s nearby environment. The product of this photoswitch is a cis-oriented, environmentally nonrelaxed chromophore that decays radiatively with a lifetime of 0.5 ns. The cis chromophore follows a photocycle similar to many bright GFP and GFP-like chromophores, decaying radiatively with a lifetime of 1.5 ns. Using pH and intensity dependent fluorescence correlation spectroscopy, we identified several dark states for HcRed that we related to the cis chromophore as follows: single-triplet transitions in microsecond time scale, protonation/deprotonation, and possibly ground-state isomerization, both in a time scale of tens of microseconds. Finally, we demonstrated identification of the trans- and cis-oriented chromophores in individual HcRed protein dimers and showed that within a single protein these conformations can occur alone or together. In the latter case, the two conformations might occur either simultaneously or alternatively due to the dimeric nature of the protein.

To a certain extent, HcRed can be considered photophysically as a mixture of both kindling proteins (e.g., asCP595) and bright GFP and GFP-like proteins (e.g., enhanced GFP, enhanced YFP or DsRed). Future mutations performed on HcRed, in particular around the chromophore site and with the purpose of completely locking the ground state into either a trans or a cis conformation may lead to better versions of kindling proteins and of bright emitting fluorescent proteins at long wavelengths.

Acknowledgment. Research carried out in part at the Center for Functional Nanomaterials, Brookhaven National Laboratory, which is supported by the U.S. Department of Energy, Division of Materials Sciences and Division of Chemical Sciences, under Contract No. DE-AC02-98CH10886 and in part, at the Center for Integrated Nanotechnologies, a U.S. Department of Energy, Office of Basic Energy Sciences user facility at Los Alamos National Laboratory (Contract DE-AC52-06NA25396) and Sandia National Laboratories (Contract DE-AC04-94AL85000). Financial support was provided in part by the laboratory directed research and development program at Los Alamos National Laboratory in New Mexico and by the research council of the Katholieke Universiteit Leuven in Belgium. RKP is financially supported by the International Iberian Nanotechnology Laboratory (INL) of Portugal. We thank Dr. K.A. Lukyanov for providing the plasmid for HcRed and Dr. Johan Hofkens (Leuven) and Dr. Jim Werner (Los Alamos) for help provided at various stages of the project.

Supporting Information Available: Supporting Information includes temperature- and pH-dependent spectra of HcRed in PBS and photon-by-photon autocorrelation of single molecule fluorescence lifetimes of HcRed. This material is available free of charge via the Internet at <http://pubs.acs.org>.

References and Notes

- (1) Tsien, R. Y. *Annu. Rev. Biochem.* **1998**, *67*, 509.
- (2) Gurskaya, N. G.; Fradkov, A. F.; Tersikh, A.; Matz, M. V.; Labas, Y. A.; Martynov, V. I.; Yanushevich, Y. G.; Lukyanov, K. A.; Lukyanov, S. A. *FEBS Lett.* **2001**, *507*, 16.
- (3) Nienhaus, G. U.; Wiedenmann, J. *ChemPhysChem* **2009**, *10*, 1369.
- (4) Tavare, J. M.; Fletcher, L. M.; Welsh, G. I. *J. Endocrinol.* **2001**, *170*, 297.
- (5) Zimmer, M. *Chem. Rev.* **2002**, *102*, 759.
- (6) Betzig, E.; Patterson, G. H.; Sougrat, R.; Lindwasser, O. W.; Olenych, S.; Bonifacio, J. S.; Davidson, M. W.; Lippincott-Schwartz, J.; Hess, H. F. *Science* **2006**, *313*, 1642.
- (7) Hofmann, M.; Eggeling, C.; Jakobs, S.; Hell, S. W. *Proc. Natl. Acad. Sci. U.S.A.* **2005**, *102*, 17565.
- (8) Andresen, M.; Stiel, A. C.; Trowitzsch, S.; Weber, G.; Eggeling, C.; Wahl, M. C.; Hell, S. W.; Jakobs, S. *Proc. Natl. Acad. Sci. U.S.A.* **2007**, *104*, 13005.
- (9) Andresen, M.; Wahl, M. C.; Stiel, A. C.; Gr, F.; SchÄfer, L. V.; Trowitzsch, S.; Weber, G.; Eggeling, C.; Grubmüller, H.; Hell, S. W.; Jakobs, S. *Proc. Natl. Acad. Sci. U.S.A.* **2005**, *102*, 13070.
- (10) Chudakov, D. M.; Feofanov, A. V.; Mudrik, N. N.; Lukyanov, S.; Lukyanov, K. A. *J. Biol. Chem.* **2003**, *278*, 7215.
- (11) Mizuno, H.; Mal, T. K.; Walchli, M.; Kikuchi, A.; Fukano, T.; Ando, R.; Jeyakanthan, J.; Taka, J.; Shiro, Y.; Ikura, M.; Miyawaki, A. *Proc. Natl. Acad. Sci. U.S.A.* **2008**, *105*, 9227.
- (12) Quillin, M. L.; Anstrom, D. A.; Shu, X. K.; O’Leary, S.; Kallio, K.; Chudakov, D. A.; Remington, S. J. *Biochemistry* **2005**, *44*, 5774.
- (13) Yarbrough, D.; Wachter, R. M.; Kallio, K.; Matz, M. V.; Remington, S. J. *Proc. Natl. Acad. Sci. U.S.A.* **2001**, *98*, 462.
- (14) Rekas, A.; Alattia, J.-R.; Nagai, T.; Miyawaki, A.; Ikura, M. *J. Biol. Chem.* **2002**, *277*, 50573.
- (15) Brejc, K.; Sixma, T. K.; Kitts, P. A.; Kain, S. R.; Tsien, R. Y.; Ormo, M.; Remington, S. J. *Proc. Natl. Acad. Sci. U.S.A.* **1997**, *94*, 2306.
- (16) Ormo, M.; Cubitt, A. B.; Kallio, K.; Gross, L. A.; Tsien, R. Y.; Remington, S. J. *Science* **1996**, *273*, 1392.
- (17) Wachter, R. M.; Elsliger, M. A.; Kallio, K.; Hanson, G. T.; Remington, S. J. *Struct. Folding Des.* **1998**, *6*, 1267.
- (18) Niwa, H.; Inouye, S.; Hirano, T.; Matsuno, T.; Kojima, S.; Kubota, M.; Ohashi, M.; Tsuji, F. I. *Proc. Natl. Acad. Sci. U.S.A.* **1996**, *93*, 13617.
- (19) Petersen, J.; Wilmann, P. G.; Beddoe, T.; Oakley, A. J.; Devenish, R. J.; Prescott, M.; Rossjohn, J. *J. Biol. Chem.* **2003**, *278*, 44626.
- (20) Wiedenmann, J.; Schenk, A.; Rocker, C.; Girod, A.; Spindler, K. D.; Nienhaus, G. U. *Proc. Natl. Acad. Sci. U.S.A.* **2002**, *99*, 11646.
- (21) Lukyanov, K. A.; Fradkov, A. F.; Gurskaya, N. G.; Matz, M. V.; Labas, Y. A.; Savitsky, A. P.; Markelov, M. L.; Zarsky, A. G.; Zhao, X.; Fang, Y.; Tan, W.; Lukyanov, S. A. *J. Biol. Chem.* **2000**, *275*, 25879.
- (22) Habuchi, S.; Ando, R.; Dedeker, P.; Verheijen, W.; Mizuno, H.; Miyawaki, A.; Hofkens, J. *Proc. Natl. Acad. Sci. U.S.A.* **2005**, *102*, 9511.
- (23) Schafer, L. V.; Groenhof, G.; Boggio-Pasqua, M.; Robb, M. A.; Grubmüller, H. *PLoS Comput Biol* **2008**, *4*, e1000034.
- (24) Nemukhin, A.; Grigorenko, B.; Savitsky, A.; Topol, I.; Burt, S. *Chem. Phys. Lett.* **2006**, *424*, 184.
- (25) Wilmann, P. G.; Petersen, J.; Pettikiriachchi, A.; Buckle, A. M.; Smith, S. C.; Olsen, S.; Perugini, M. A.; Devenish, R. J.; Prescott, M.; Rossjohn, J. *J. Mol. Biol.* **2005**, *349*, 223.
- (26) Subramaniam, V.; Hanley, Q. S.; Clayton, A. H. A.; Jovin, T. M. In *Biophotonics*, Part A; Academic Press Inc: San Diego, CA, 2003; Vol. 360, p 178.
- (27) Widengren, J.; Mets, U.; Rigler, R. *Chem. Phys.* **1999**, *250*, 171.
- (28) Cotlet, M.; Hofkens, J.; Habuchi, S.; Dirix, G.; Van Guyse, M.; Michiels, J.; Vanderleyden, J.; De Schryver, F. C. *Proc. Natl. Acad. Sci. U.S.A.* **2001**, *98*, 14398.
- (29) Maus, M.; Cotlet, M.; Hofkens, J.; Gensch, T.; De Schryver, F. C.; Schaffer, J.; Seidel, C. A. M. *Anal. Chem.* **2001**, *73*, 2078.
- (30) Enderlein, J.; Goodwin, P. M.; VanOrden, A.; Ambrose, W. P.; Erdmann, R.; Keller, R. A. *Chem. Phys. Lett.* **1997**, *270*, 464.
- (31) Kohl, T.; Schwille, P. *Adv. Biochem. Eng./Biotechnol.* **2005**, *95*, 107.
- (32) Cotlet, M.; Goodwin, P. M.; Waldo, G. S.; Werner, J. H. *ChemPhysChem* **2006**, *7*, 250.
- (33) Chen, Y.; Muller, J. D.; Ruan, Q. Q.; Gratton, E. *Biophys. J.* **2002**, *82*, 133.
- (34) Schwille, P.; Kummer, S.; Heikal, A. A.; Moerner, W. E.; Webb, W. W. *Proc. Natl. Acad. Sci. U.S.A.* **2000**, *97*, 151.
- (35) Heikal, A. A.; Hess, S. T.; Baird, G. S.; Tsien, R. Y.; Webb, W. W. *Proc. Natl. Acad. Sci. U.S.A.* **2000**, *97*, 14831.
- (36) Haupts, U.; Maiti, S.; Schwille, P.; Webb, W. W. *Proc. Natl. Acad. Sci. U.S.A.* **1998**, *95*, 13573.
- (37) Hendrix, J.; Flors, C.; Dedeker, P.; Hofkens, J.; Engelborghs, Y. *Biophys. J.* **2008**, *94*, 4103.
- (38) Gross, L. A.; Baird, G. S.; Hoffman, R. C.; Baldrige, K. K.; Tsien, R. Y. *Proc. Natl. Acad. Sci. U.S.A.* **2000**, *97*, 11990.
- (39) Heim, R.; Prasher, D. C.; Tsien, R. Y. *Proc. Natl. Acad. Sci. U.S.A.* **1994**, *91*, 12501.
- (40) Schafer, L. V.; Groenhof, G.; Klingen, A. R.; Ullmann, G. M.; Boggio-Pasqua, M.; Robb, M. A.; Grubmüller, H. *Angew. Chem., Int. Ed.* **2007**, *46*, 530.
- (41) Battad, J. M.; Wilmann, P. G.; Olsen, S.; Byres, E.; Smith, S. C.; Dove, S. G.; Turcic, K. N.; Devenish, R. J.; Rossjohn, J.; Prescott, M. J. *Mol. Biol.* **2007**, *368*, 998.
- (42) Lessard, G. A.; Habuchi, S.; Werner, J. H.; Goodwin, P. M.; De Schryver, F.; Hofkens, J.; Cotlet, M. *J. Biomed. Opt.* **2008**, *13*.
- (43) Cotlet, M.; Hofkens, J.; Kohn, F.; Michiels, J.; Dirix, G.; Van Guyse, M.; Vanderleyden, J.; De Schryver, F. C. *Chem. Phys. Lett.* **2001**, *336*, 415.
- (44) Lounis, B.; Deich, J.; Rosell, F. I.; Boxer, S. G.; Moerner, W. E. *J. Phys. Chem. B* **2001**, *105*, 5048.

- (45) Schuttrigkeit, T. A.; Zachariae, U.; von Feilitzsch, T.; Wiehler, J.; von Hummel, J.; Steipe, B.; Michel-Beyerle, M. E. *ChemPhysChem* **2001**, *2*, 325.
- (46) Wilmann, P. G.; Turcic, K.; Battad, J. M.; Wilce, M. C. J.; Devenish, R. J.; Prescott, M.; Rossjohn, J. *J. Mol. Biol.* **2006**, *364*, 213.
- (47) Habuchi, S.; Cotlet, M.; Gensch, T.; Bednarz, T.; Haber-Pohlmeier, S.; Rozenski, J.; Dirix, G.; Michiels, J.; Vanderleyden, J.; Heberle, J.; De Schryver, F. C.; Hofkens, J. *J. Am. Chem. Soc.* **2005**, *127*, 8977.
- (48) Chatteraj, M.; King, B. A.; Bublit, G. U.; Boxer, S. G. *Proc. Natl. Acad. Sci. U.S.A.* **1996**, *93*, 8362.
- (49) Liu, Y.; Kim, H. R.; Heikal, A. A. *J. Phys. Chem. B* **2006**, *110*, 24138.
- (50) Loos, D. C.; Habuchi, S.; Flors, C.; Hotta, J. I.; Wiedenmann, J. R.; Nienhaus, G. U.; Hofkens, J. *J. Am. Chem. Soc.* **2006**, *128*, 6270.
- (51) Rizzo, M. A.; Springer, G. H.; Granada, B.; Piston, D. W. *Nat. Biotechnol.* **2004**, *22*, 445.
- (52) Kneen, M.; Farinas, J.; Li, Y. X.; Verkman, A. S. *Biophys. J.* **1998**, *74*, 1591.
- (53) Elslinger, M. A.; Wachter, R. M.; Hanson, G. T.; Kallio, K.; Remington, S. J. *Biochemistry* **1999**, *38*, 5296.
- (54) Bizzarri, R.; Nifosi, R.; Abbruzzetti, S.; Rocchia, W.; Guidi, S.; Arosio, D.; Garau, G.; Campanini, B.; Grandi, E.; Ricci, F.; Viappiani, C.; Beltram, F. *Biochemistry* **2007**, *46*, 5494.
- (55) Bizzarri, R.; Arcangeli, C.; Arosio, D.; Ricci, F.; Faraci, P.; Cardarelli, F.; Beltram, F. *Biophys. J.* **2006**, *90*, 3300.
- (56) Wilmann, P. G.; Battad, J.; Beddoe, T.; Olsen, S.; Smith, S. C.; Dove, S.; Devenish, R. J.; Rossjohn, J.; Prescott, M. *Photochem. Photobiol.* **2006**, *82*, 359.
- (57) Widengren, J.; Schwille, P. *J. Phys. Chem. A* **2000**, *104*, 6416.
- (58) Yang, H.; Xie, X. S. *J. Chem. Phys.* **2002**, *117*, 10965.
- (59) Dickson, R. M.; Norris, D. J.; Tzeng, Y. L.; Moerner, W. E. *Science* **1996**, *274*, 966.
- (60) Dickson, R. M.; Norris, D. J.; Tzeng, Y. L.; Sakowicz, R.; Goldstein, L. S. B.; Moerner, W. E. In *Molecular Crystals and Liquid Crystals Science and Technology Section A-Molecular Crystals and Liquid Crystals*. Gordon Breach Sci Publ Ltd: Berkshire, England, 1996; pp 31–39.

JP9102146